This is the peer reviewed author accepted manuscript (post print) version of a published work that appeared in final form in:

Diquattro, Stefania, Garau, Giovanni, Mangia, Nicoletta P., Drigo, Barbara, Lombi, Enzo, Vasileiadis, Sotirios, Castaldi, Paola 2020 'Mobility and potential bioavailability of antimony in contaminated soils: Short-term impact on microbial community and soil biochemical functioning', Ecotoxicology and Environmental Safety, vol. 196, article no. 110576, pp. 1-10

This output may not exactly replicate the final published authoritative version for which the publisher owns copyright. It is not the copy of record. This output may be used for non-commercial purposes. This version is licensed under a Creative Commons CC-BY-NC-ND 4.0 license (http://creativecommons.org/licenses/by-nc-nd/4.0/).

The final definitive published version (version of record) is available at: https://doi.org/10.1016/j.ecoenv.2020.110576

Persistent link to the UniSA Research Outputs Repository: https://researchoutputs.unisa.edu.au/11541.2/142233

General Rights

Copyright and moral rights for the publications made accessible in the UniSA Research Outputs Repository are retained by the authors and/or other copyright owners and it is a condition of accessing publications that users recognize and abide by the legal requirements associated with these rights.

- Users may download and print one copy for the purpose of private study or research.
- You may not further distribute the material or use it for any profit-making activity or commercial gain
- You may freely distribute the persistent link identifying the publication in the UniSA Research Outputs Repository

If you believe that this document breaches copyright, please contact us and provide details. We will remove access to the work immediately and investigate your claim.

Mobility and potential bioavailability of antimony in contaminated soils: Short-term impact on microbial community and soil biochemical functioning

Stefania Diquattro[a] Giovanni Garau[a] Nicoletta P.Mangia[a] BarbaraDrigo[b] EnzoLombi[b] SotiriosVasileiadis[c] PaolaCastaldi[a]

[a] Dipartimento di Agraria, University of Sassari, Viale Italia 39, 07100, Sassari, Italy

[b]Future Industries Institute, University of South Australia, Mawson Lakes, SA, 5095, Australia[c] Department of Biochemistry and Biotechnology, Lab of Plant and Environmental Biotechnology, University of Thessaly, Viopolis, 41500, Larissa, Greece

Abstract

Antimony (Sb) and its compounds are emerging priority pollutants which pose a serious threat to the environment. The aim of this study was to evaluate the short-term fate of antimonate added to different soils (S1 and S2) with respect to its mobility and impact on soil microbial communities and soil biochemical functioning. To this end, S1 (sandy clay loam, pH 8.2) and S2 (loamy coarse sand, pH 4.9) soils were spiked with 100 and 1000 mg Sb(V) kg^{-1} soil and left in contact for three months. Sequential extractions carried out after this contact time indicated a higher percentage of labile antimony in the Sb-spiked S1 soils than S2 (e.g. ~13 and 4% in S1 and S2 treated with 1000 mg Sb(V) kg^{-1} respectively), while the opposite was found for residual (hardly bioavailable) Sb. Also, a reduced number of culturable heterotrophic bacteria was recorded in Sb-spiked S1 soil (compared to the unpolluted S1), while an increased one was found in S2. Heterotrophic fungi followed the opposite trend. Actinomycetes and heat-resistant aerobic bacterial spores showed a variable trend depending on the soil type and Sb(V) treatment. The Biolog community level physiological profile indicated a reduced metabolic activity potential of microbial communities from the Sb-spiked S1 soils (e.g. <50% for Sb-1000 compared to the unpolluted S1), while an increase was recorded for those extracted from the Sb-spiked S2 soils (e.g. >2-fold for Sb-1000). The soil dehydrogenase activity followed the same trend. High-throughput 16S rRNA amplicon sequencing analysis revealed that Sb did not influence the bacterial α-diversity in both soils, while significantly affected the composition of the respective soil bacterial communities. Several phyla (e.g. *Nitrosospira Nitrososphaeraceae*, *Adheribacter*) were found positively correlated with the concentration of water-soluble Sb in soil. Overall, the results obtained suggest that the risk assessment in soils polluted with antimony should be a priority especially for alkaline soils where the high mobility of the anionic $Sb(OH)_6^-$ species can pose, at least in the short-term, a serious threat for soil microbial abundance, diversity and functionality, soil fertility and eventually human health.

Keywords

Sb(V)

Sequential extraction

Culturable heterotrophic microorganisms

Community level physiological profile

Soil dehydrogenase activity

High-throughput 16S rRNA amplicon sequencing

1. Introduction

Antimony (Sb) and its derivative compounds, listed as priority pollutants by the European Union and the United States Environmental Protection Agency (CEC, 1998; US EPA, 2009), are becoming increasingly widespread in the environment mainly due to anthropogenic activities (Tandy et al., 2017). High antimony levels in soil can be commonly due to high vehicular traffic, recreational shooting or mining activities (Tandy et al., 2017; Földi et al., 2018; Cidu et al., 2013). Antimony can exists in different oxidation states (i.e. −3, 0, +3, +5) even if, in aqueous and soil systems, it mainly occurs as trivalent Sb(III) and/or pentavalent Sb(V) inorganic species; antimonite [$Sb(OH)_3$] and antimonate [$Sb(OH)_6^-$] are the most common Sb(III) and Sb(V) compounds respectively in a wide pH range (Filella et al., 2002a, 2002b; Herath et al., 2017). Sb(V) dominates in oxygenated natural waters and aerated soils and seems less toxic, but more mobile, than Sb(III) (Herath et al., 2017). However, as emphasized by Filella et al. (2009), the relative toxicity of the two antimony species depends on different factors (e.g. the target organism, the route of exposure, the co-occurrence of other contaminants), and clear evidence on the higher Sb(III) toxicity are currently missing. In soil systems, the mobility of Sb(V) is largely controlled by the pH (Nakamaru et al., 2006), i.e. the Sb(V) mobility increases at higher pH values. This is mainly because of the electrostatic

repulsion phenomena occurring between the $Sb(OH)_6^-$ oxoanion and the negatively charged surface groups of clays, Fe or Al hydrous oxides and organic matter in soil. Moreover, sequential extractions carried out in different studies also indicated that Sb tends to be associated with Fe or Al hydrous oxides or adsorbed by humic acids (Garau et al., 2017; Diquattro et al., 2018; Steely et al., 2007).

The assessment of mobile or labile (i.e. readily soluble and potentially bioavailable) Sb species in soil is of utmost importance since, as for other potentially toxic trace elements (PTTE), this is expected to negatively correlate with the abundance, diversity and functioning of soil microbiota (e.g. Luo et al., 2014; Garau et al., 2019a). This also implies that, for a thorough assessment of the Sb impact in polluted soils, comprehensive microbial and biochemical analyses should always accompany soil chemical determinations. For instance, it was shown that the size of culturable heterotrophic bacterial populations was very sensitive to critical concentrations of labile PTTE in soil (Wang et al., 2011; Courtin-Nomade et al., 2012; Garau et al., 2007, 2019a). Likewise, soil dehydrogenase activity was often negatively correlated with labile contaminants in soil and can be of help in the assessment of the environmental status of polluted areas (e.g. Garau et al., 2019a). Moreover, labile PTTE in soil can significantly modify the C-source utilisation of the resident microbial communities as previously showed using the Biolog community level physiological profile approach (Garau et al., 2007, 2017). Finally, labile contaminants in soil can also influence the structure of the resident microbial community and this can have relevant effects on its resilience to external changes (Guillamot et al., 2014; Li et al., 2016), such as for instance the spread of antibiotic resistance (Chen et al., 2019). In this context, modern DNA sequencing technologies such as Illumina high-throughput 16S rRNA gene amplicon sequencing, can be particularly useful at revealing the impact of PTTE on the structure and diversity of soil microbial community (e.g. Garau et al., 2017). Despite the relevance of such aspects, the fate of Sb in contaminated soils was often studied only on

a chemical basis, whilst its impact on the soil microbial component and biochemical status was rarely addressed especially in the short-term (Wang et al., 2011; Wang et al., 2018; Courtin-Nomade et al., 2012). More in general, "the real environmental risk posed by antimony is still largely in need of assessment and proof" as pointed out almost ten years ago (Filella et al., 2009).

The aim of the present work was therefore to evaluate the short-term fate of antimonate, added at two different concentrations, on two distinct soils, with respect to its mobility and potential bioavailability, as well as to its impact on selected soil microbial and biochemical features. In particular, sequential extractions, culturable microbial populations, dehydrogenase activity, Biolog community level physiological profile and bacterial community structure (high-throughput 16S rRNA gene amplicon sequencing with the Illumina technology) were investigated to gain a deeper understanding of the chemical and (micro)biological impact of Sb in contaminated soils.

2. **Materials and methods**

2.1. **Soil sampling and physico-chemical characteristics**

Random topsoil samples (0–20 cm depth; S1 and S2) were collected (with sterile auger soil samplers) during summer 2016 from two different sites (approx. 300 m^2 each) in Sardinia (Italy), both located in the north-western area (soil S1: 40°43′32.77″N 8°24′48.6″E; soil S2: 40°56′15.7″N 8°53′30.4″E). The soils from these sites, which were approx. 45 km apart, were selected because: i) they were historically not used for agricultural or anthropogenic activities; ii) they were far from any industrial plants or other possible contamination sources; iii) they had different physico-chemical properties. The collected soil samples were bulked according to their site of origin and sieved to <2 mm before physico-chemical analyses and mesocosms set up. In particular, according to particle-size analysis, carried out using the pipette method

(Day, 1965), S1 was a sandy clay loam while S2 was a loamy coarse sand (USDA classification). Moreover, S1 and S2 soils were subjected to the following chemical analyses: electric conductivity (EC) and pH were both determined in soil suspensions (1:2.5 soil: deionised water ratio) (Gazzetta Ufficiale n. 248 del 21 ottobre 1999); total and active carbonates were determined by acid dissolution (volumetric calcimeter method) and by reaction of soil with 0.1 M ammonium oxalate respectively (Gazzetta Ufficiale n. 248 del 21 ottobre 1999); total organic carbon and nitrogen were determined by means of a CHN analyser (Leco CHN 628) with an oat meal Leco part n. 502e276 as calibration sample; total P was determined spectrophotometrically (ascorbic acid method) after soil mineralisation (Gazzetta Ufficiale n. 248 del 21 ottobre 1999); available P was determined by extraction with sodium bicarbonate (Olsen method, Gazzetta Ufficiale n. 248 del 21 ottobre 1999); dissolved organic carbon (DOC) was estimated as described by Brandstetter et al. (1996); the point of zero charge (pH_{PZC}) was determined by potentiometric titration as described in Appel et al. (2003); cation exchange capacity (CEC) was determined using the $BaCl_2$ and triethanolamine method (Gazzetta Ufficiale n. 248 del 21 ottobre 1999); metals and antimony in soils were quantified using a flame atomic absorption spectrometer (FAAS; PerkinElmer AAnalyst 200) or a graphite furnace atomic absorption spectrometer (GFAAS; PerkinElmer AAnalyst 400-HGA 900, Software AA-WinLab32) after soil digestion with aqua regia reverse solution (HNO_3/HCl 3:1 ratio) and microwave mineralisation (Milestone MLS1200). FAAS and GFAAS were used to determine the content of soil metals and antimony respectively.

2.2. **Mesocosms set up and Sb(V)-spiking experiment**

Each of the two soils (S1 and S2) was used to set up a total of 9 soil mesocosms (5 kg each, dry weight equivalent) arranged in brand new plastic pots (50 × 20 × 20 cm, L x W x H) which were washed with deionised water before use. Soil mesocosms randomly received one of the

following treatments: no Sb(V) added (control soil; S); 100 mg Sb(V) kg^{-1} soil (S-100); 1000 mg Sb(V) kg^{-1} soil (S-1000). The Sb concentrations applied were selected to mimic the range of Sb contamination that can occur in mining soils, i.e. a medium-low (100 mg kg^{-1}) and a high (1000 mg kg^{-1}; e.g.) pollution level (e.g. Courtin-Nomade et al., 2012; Cidu et al., 2013; Garau et al., 2017). Each treatment was applied in triplicate mesocosms. Soil spiking with antimony was carried out using Sb(V) solutions deriving from $KSb(OH)_6 \cdot 7\ H_2O$ (CAS 12208-13-8; Merck), which were added to soils to reach a final contamination level of 100 and 1000 mg Sb(V) kg^{-1} soil. All soils were then brought to 60% of their water holding capacity (WHC) with deionised water. Before addition to a soil, each Sb(V) solution was brought to the same pH of the soil using 0.1 M NaOH/HCl solutions. After Sb spiking, treated and untreated (control) soils were left for 3 months at 25 °C during which they were periodically mixed (once every two weeks) and the water content maintained constant (60% WHC). Based on previous studies (Murata et al., 2005; Wang et al., 2011; Guillamot et al., 2014), this time-period was deemed suitable to highlight possible short-term impact of Sb on soil microbial community and soil biochemical functioning.

2.3. **Sequential extraction of Sb in soil mesocosms**

After three months of contact, the total content of Sb in spiked soils was determined by GFAAS as previously described. The recovery rate of Sb in such spiked soils was 97–103%. Sb mobility was evaluated through the sequential extraction procedure of Wenzel et al. (2001) with minor modifications. This method, originally developed for arsenic, is widely used for the sequential extraction of antimony (e.g. Garau et al., 2017; Diquattro et al., 2018; Földi et al., 2018; Ngo et al., 2020) because of the similar geochemical behaviour of these metalloids (Wilson et al., 2010). Briefly, triplicate soil samples (1 g) from each contaminated mesocosm were sequentially treated with 25 mL of different extraction reagents. After each extraction step, soil

suspensions were centrifuged at 3000 rpm for 10 min and filtered through 0.45 μm cellulose acetate filters. The Sb in filtered solutions was quantified by GFAAS (PerkinElmer AAnalyst 400-HGA 900, Software AA-WinLab32). Soil samples were sequentially treated with the following extractants: water (2h, 130 rpm, 20 °C), to estimate the water-soluble Sb (Step 0, additional step with respect to the original extraction procedure); 0.05 M $(NH_4)_2SO_4$ solution (4h, 130 rpm, 20 °C), to assess the non-specifically adsorbed Sb fraction (Step 1); 0.05 M $(NH_4)H_2PO_4$ (16h, 130 rpm, 20 °C) to extract the Sb pool specifically-sorbed (Step 2); 0.2 M ammonium oxalate solution pH 3.25 (4h, 130 rpm in the dark, 20 °C; Step 3) followed by 0.2 M ammonium oxalate solution+0.1 M ascorbic acid pH 3.25 (30 min in a water basin at 96 °C; Step 4) to extract the Sb associated to amorphous (Step 3) and crystalline (Step 4) Al- and Fe-oxides respectively. The residual Sb was calculated by difference, i.e. total Sb in soil minus Sb extracted in steps 1–4.

2.4. **Soil microbial and biochemical analyses**

After the three months incubation, total culturable heterotrophic bacteria, fungi, actinomycetes, and the number of heat-resistant aerobic bacterial spores (e.g. *Bacillus* spp.) were enumerated in triplicate soil samples from the different mesocosms using the ten-fold serial dilution and spread plate method as previously described (Chessa et al., 2016). The growth media used to quantify the different microbial populations were as follow: 1:10 TSB (Tryptic Soy Broth, Microbiol, Cagliari, Italy) + agar (1.5%) for soil heterotrophic bacteria and aerobic bacterial spores; GYEP pH 4.7 (Glucose Yeast Extract Peptone medium; Garau et al., 2007) for soil fungi; AIA (Actinomycete Isolation Agar, Difco, Milan, Italy) for actinomycetes. Soil samples (10 g) were dispersed in 90 mL of sodium pyrophosphate solution (2 g L^{-1}) and serial ten-fold dilutions were obtained using 0.89% NaCl solution. Agar plates were then inoculated with 100 μL of the different ten-fold dilutions and incubated at 28 °C for 3 days until colony count.

To enumerate heat-resistant aerobic bacterial spores, the ten-fold dilutions were heat-treated (80 °C × 15 min) before plate inoculation. The microbial abundance in each soil was expressed as Log_{10} CFU (Colony Forming Unit) g^{-1} soil (dry weight basis).

The microbial community structure of Sb-spiked and control soils was investigated through the Biolog community level physiological profile (CLPP) using Biolog EcoPlates™ (Biolog Inc., Hayward, CA). Microbial communities were extracted from triplicate soil samples (10 g each) deriving from respective (treated and untreated) mesocosms as previously described (Garau et al., 2007) with minor modifications. Briefly, 30 mL of the 100-fold dilution used for the enumeration of culturable microorganisms were centrifuged for 5 min at 700 rpm and the clear supernatant was used to inoculate the wells of the Biolog EcoPlate™ (120 µL per well). The Biolog EcoPlates™ are ready to use 96 wells microtiter plates containing in each well a different carbon source of soil/environmental relevance (Insam et al., 1997). A total of 31 different carbon sources and a control well with no carbon (all replicated three times) are present in each Biolog EcoPlate™. A tetrazolium dye is also incorporated in the plate wells to reveal oxidative catabolism (i.e. carbon source utilisation) as purple colour formation. Inoculated plates were incubated at 28 °C for 7 days and purple colour formation in each well was recorded daily by measuring the absorbance at 590 nm (OD_{590}), using an automatic Biolog MicroStation™ reader. Data analysis was carried out as follows: all the OD_{590} values were first blanked against the respective time 0 readings and further subtracted against the respective control well (with no carbon source). Finally, they were processed to obtain a measurement of the potential catabolic activity of the microbial community, i.e. the average well colour development (AWCD). This latter was calculated as follow: $AWCD = [\Sigma (R-C)] / 31$ where C represents the absorbance value of control wells, R is the mean absorbance of the response wells, and 31 is the number of carbon substrates in the plate. The richness value, or the number of substrates catabolised by each microbial community, was also determined as the number of

wells with OD_{590} > than 0.15 (Garau et al., 2007). AWCD and richness values reported refer to the 120 h incubation time as this time-point provided the best discrimination between treatments. All OD_{590} values were further subjected to Principal Component Analysis (PCA) to investigate possible difference in C-source consumption by the different soil microbial communities. PCA was carried out using the Past software v. 3.25 (Hammer et al., 2001).

Soil dehydrogenase activity (DHG) was determined colorimetrically in triplicate soil samples collected from each mesocosm. Soil samples (10 g) were treated with a triphenyltetrazolium chloride solution and leaved for 24 h at 30 °C as described by Alef and Nannipieri (1995). The DHG activity was then quantified spectrophotometrically in the liquid phase (OD_{480} nm) and expressed as triphenyl formazan (TPF) formed per g^{-1} soil (dry weight basis).

2.5. **Molecular analysis of soil bacterial communities**

After the three months incubation, total DNA was extracted from each soil mesocosm (~500 mg) using the PowerSoil DNA isolation Kit (Mo Bio laboratories, Carlsbad, CA) according to the manufacturer's instructions. The 16S rRNA gene amplification and amplicon sequencing was performed at the Integrated Microbiome Resource (IMR, Halifax, NS, Canada) facilities according to the service provider's published protocol (Walters et al., 2015) with the Earth Microbiome Project consortium (Gilbert et al., 2018) V4-5 hypervariable regions suggested 515f-926r (Walters et al., 2015; Parada et al., 2016) primer set (515f 5′-GTGYCAGCMGCCGCGGTAA-3′, 926r 5′-CCGYCAATTYMTTTRAGTTT-3′).

2.6. **Microbiome bioinformatics**

The retrieved per sample sequence read-pairs were quality trimmed with Trimmomatic v0.36 (Bolger et al., 2014) using the default settings (with the exception of 5’ trimming) and a minimum length cutoff of 150 bp after the sample index trimming (the average amplicon length was 292 bp). The original amplicon sequences were reconstructed through assembly of the read

pairs with the FLASH v1.2.11 (Magoč and Salzberg, 2011) software allowing a 5% mismatch/overlap ratio and a minimum overlap of 10 bp. Further sequence screening for sequencing errors and PCR introduced chimeras, alignment to reference databases, and generation of operational taxonomic unit (OUT) matrices was performed with the Mothur v1.41.3 (Schloss et al., 2009) software suit as briefly described here. The reconstructed amplicon sequences were clustered via global alignment in a pairwise manner at ~99% identity to the longest sequence per cluster, thus, assuming an ~1% sequencing error rate (Schloss et al., 2009). The sequences were then aligned against the Silva v132 16S rRNA gene reference alignment database and sequences failing to align were considered non-specific and were removed from downstream analysis. Chimeric amplicons were identified and removed using the abundance-based de novo UCHIME v4.2 (Edgar et al., 2011) approach. A further step of classification, using the naïve Bayesian classifier (Wang et al., 2007) as implemented in Mothur, was performed for identifying and further removing sequences classified in non-target taxa (unknown, eukaryotic, chloroplasts and mitochondria). Sequence distances were calculated for the remaining aligned sequences, while clustering of sequences into 0.03 distance defined operational taxonomic units (OTUs) was performed with the recently developed OptiClust algorithm (Westcott and Schloss, 2017).

2.7. **Statistical analysis**

Sequencing effort coverage and α-diversity indices were calculated with the Entropart v1.5–3 (Marcon and Hérault, 2015) and the Vegan v2.5–4 (Oksanen et al., 2018) packages of the R v3.5.1 (R Core Team, 2017) software with Vegan being used also for the multivariate approaches described below. The Good's coverage estimate (Good, 1953) was used for assessing the achieved sequencing depth. The implemented measures of α-diversity were: the Shannon index (1st order diversity, representative of less dominant OTUs); the reciprocal

Simpson index (Jost, 2006) (2nd order diversity, indicative of more dominant OTUs); the Fisher's α (Fisher et al., 1943) index (indicative of the most dominant OTU diversity); the observed richness (S), the Chao1 (Chao, 1984), and the Abundance-based Coverage Estimator (ACE; Chao, 1987) richness estimators (representative of identified/estimated number of OTUs, or, zero order diversity). One-way analysis of variance (ANOVA) (using the interactions of the soil and applied Sb levels as groups as delineated in the plots) and Tukey's post-hoc analysis, or their non-parametric equivalents (Kruskal-Wallis test followed by the Wilcoxon rank sum test), were implemented for assessing statistically significant differences between the tested groups using the Agricolae v3.5.2 package (de Mendiburu, 2016) of the R software.

The data were further transformed using the Hellinger transformation method (Legendre and Gallagher, 2001) and were used for performing principal components analysis (PCA) and its canonical version, namely, redundancy analysis (RDA). RDA was selected according to the detrended correspondence analysis (DCA) test as previously suggested (Lepš; Šmilauer, 2003). To this end, a 1st DCA axis length value being lower than 3 standard deviations, suggests linear OTU gradients which are best represented by methods like RDA. Permutational analysis of variance (PERMANOVA) (Anderson, 2017) tests accompanied the RDA for obtaining the tested model explained variances and *P*-values, and were performed using 999 permutations. Treatment-wise differentially abundant OTUs were identified with the non-parametric ANOVA equivalent, Kruskal-Wallis test, followed by the pairwise comparison Wilcoxon rank sum test (if the Kruskal Wallis test was significant) as previously suggested (Weiss et al., 2017).

Sequential extraction and microbial and biochemical data were subjected to one-way ANOVA. When significant *P* values were obtained ($P < 0.05$) differences between individual means

were compared with the post-hoc Tukey Kramer multiple comparison test ($P < 0.05$) using the NCSS software (Keysville, Utah).

3. **Results and discussion**

3.1. **Soil characterisation and sequential extraction of Sb from contaminated soils**

The S1 soil (sandy clay loam) was alkaline (pH 8.2) while S2 (loamy coarse sand) was acidic (pH 4.9). Moreover, S1 had a higher CEC compared to S2, while the opposite was true for SOM and DOC (Table 1). High concentrations of total Fe and Al were recorded in both soils (especially in S1) while total Ca was much more abundant in S1 (62,500 mg kg^{-1}) with respect to S2 (48 mg kg^{-1}) (Table 1). Antimony was not detected in any of the two soils (i.e. Sb < 1 mg kg^{-1}).

Table 1. Selected physico-chemical characteristics of the uncontaminated soils used in this study.

Physico-chemical parameters	**S1 soil**	**S2 soil**
pH(H_2O)	8.22 ± 0.1	4.91 ± 0.2
EC (µS cm^{-1})	378 ± 8	327 ± 4
DOC (mg g^{-1})	0.17 ± 0.00	0.39 ± 0.02
SOM (%)	1.75 ±	2.19 ±
Total carbonates (g kg^{-1})	300 ± 1.27	12 ± 0.28
Active carbonate (g kg^{-1})	82 ± 0.91	11 ± 0.44
Total P (mg kg^{-1})	330 ± 26	272 ± 34

Physico-chemical parameters	**S1 soil**	**S2 soil**
Available P (mg kg^{-1})	31 ± 2.6	56 ± 1.4
CEC ($cmol_{(+)}$ kg^{-1})	21.1 ± 0.8	12.9 ± 2.5
pH_{PZC}	5.7	2.6
Texture (USDA)	Sandy clay loam	Loamy coarse sand
Total metals and antimony (mg kg^{-1})		
Fe	16,350 ± 1061	5650 ± 71
Mn	174 ± 16	87 ± 2
Na	2150 ± 636	750 ± 71
K	7100 ± 707	1500 ± 139
Mg	3100 ± 283	770 ± 14
Ca	62,500 ± 2828	2426 ± 145
Al	19,930 ± 1018	3924 ± 749
Sb	n.d.[a]	n.d.

289 a

290 n.d., not detected (i.e. < 1 mg kg^{-1} soil).

291 To investigate the mobility of antimony in soils after three months since spiking, we used the
292 sequential extraction procedure of Wenzel et al. (2001) slightly modified as previously
293 described. The percentage of water-soluble (i.e. highly bioavailable) antimony (Step 0)
294 extracted from S1 polluted soils (~13% of total Sb in both S1-100 and −1000) was higher than
295 that recorded in S2 polluted ones (~10 and 4% in S2-100 and −1000 respectively) (Fig. 1). This

could be mainly due to the S1 higher pH value that implies: i) a greater competition between hydroxide (OH^-) and $Sb(OH)_6^-$ anions for Sb retention sites (Rakshit et al., 2015) and ii) a higher repulsion between the $Sb(OH)_6^-$ anions and the negatively charged soil surfaces.

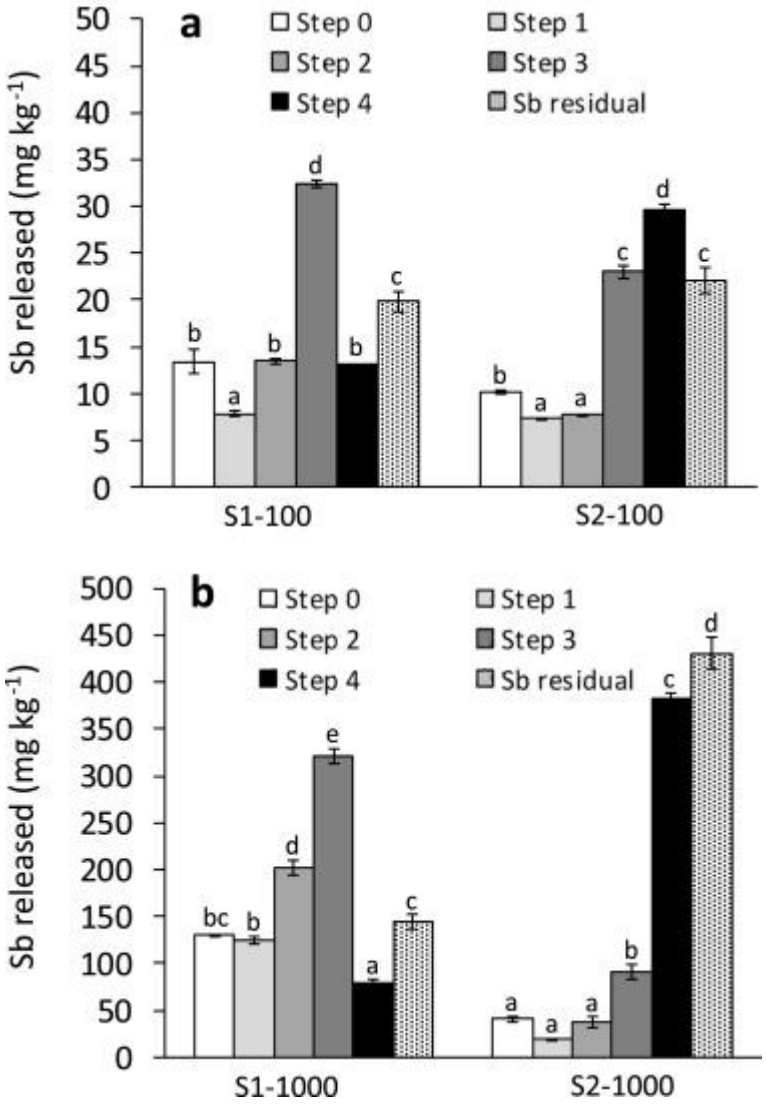


Fig. 1. Sb sequentially extracted from soils spiked with 100 (S-100) (a) and 1000 (S-1000) mg Sb(V) Kg^{-1} soil (b). For each soil type (i.e. S1 and S2) and contamination level, different letters on top of each bar denote statistically significant differences ($P < 0.05$).

Also, the exchangeable (and relatively bioavailable) Sb fraction (Step 1) was higher in S1 (7.9 and 12.5% of total Sb in S1-100 and −1000 respectively) than in S2 (7.4 and 1.9% in S2-100 and −1000 respectively). However, statistically significant differences were only observed at

307 the higher Sb concentration (Fig. 1). The similar amount of Sb released in this step in the S2-
308 100 (7.4 mg kg^{-1}) and S2-1000 (19 mg kg^{-1}) treatments suggested a more limited anion
309 exchange capacity of S2 soil (compared to S1). Apparently, this was not the case of S1 where
310 the Sb released in Step 1 increased from 7.9 mg kg^{-1} to 125 mg kg^{-1} in S1-100 and S1-1000
311 respectively. Even if S1 is alkaline, and this generally limits the electrostatic interaction of
312 antimonate [$Sb(OH)_6^-$] with the negatively charged surface of soil colloids, it contains a higher
313 quantity of clay (21 vs. 10% of S2) and it is characterised by a higher CEC with respect to S2
314 (Table 1). As shown in other studies for phosphate and arsenate, this could imply the higher
315 occurrence in S1 of ternary complexation phenomena in which polyvalent metal cations (e.g.,
316 Ca, Fe and Al) act as bridging elements between the negatively charged functional groups of
317 clays or organic matter and the antimonate anion (Diquattro et al., 2018; Filella and Williams,
318 2012). Moreover, given the higher content of total Fe and Al in S1, it could be hypothesised in
319 such soil a greater presence of Fe/Al oxides and oxy-hydroxides which are generally
320 characterised by high values of point of zero charge (i.e. > 8.2). This could have favoured the
321 formation of electrostatic bonds between surficial OH_2^+ of Fe/Al oxides and oxy-hydroxides
322 with the Sb(V) oxyanion, contributing to explain the higher content of exchangeable Sb in S1
323 soil.
324 A similar trend was detected for the specifically-sorbed Sb forming inner-sphere complexes
325 with the soil components (Step 2). This Sb pool can be considered as relatively bioavailable
326 since it can be easily mobilised following a local pH change and/or a variation of P
327 concentration (Wenzel et al., 2001). The Sb extracted in Step 2 was 13.5 and 20.2% of total Sb
328 for S1-100 and −1000, and 7.8 and 3.7% in S2-100 and −1000 respectively (Fig. 1).
329 More than 40% of total antimony was extracted in both soils in Step 3 and Step 4 (Fig. 1).
330 These latter steps accounted for the Sb fractions retained by amorphous and crystalline Fe/Al
331 oxides (and/or oxy-hydroxides) respectively.

The residual antimony, i.e. the fraction strongly retained in soil and hardly bioavailable, was higher in S2 (22 and 43% of total Sb in S2-100 and −1000 respectively) than in S1 (20 and 14% in S1-100 and −1000 respectively) (Fig. 1). The higher amount of residual antimony recorded in S2 soil (especially in S2-1000) could be ascribed to its low pH (i.e. 4.9) which could have promoted the formation of stable precipitates between Sb(V) and soluble Al^{3+} or Fe^{3+}, e.g. $FeSbO_4$ and $AlSbO_4$ (Dousova et al., 2018; Herath et al., 2017; Vandenbohede et al., 2019). However, given that residual Sb was calculated by subtracting that extracted in Steps 0–4 from total Sb in soil, these data may require further investigation.

Overall, the results of the sequential extractions showed that the short-term fate of Sb(V) was largely influenced by selected soil physico-chemical properties such as pH and Al and Fe hydroxides content as well as SOM and clay content.

3.2. Influence of Sb on soil culturable microorganisms

After three months since Sb spiking, the bacterial number decreased significantly in S1 soils treated with Sb(V) compared to control (~25 and 50% lower in S1-100 and −1000 respectively), while an opposite trend was recorded for S2 soil (~50% higher in both S2-100 and −1000) (Table 2). Contrasting trends were also noticed for fungi, whose number significantly increased in S1 soils spiked with Sb(V) (~60 and 90% higher in S1-100 and −1000 respectively), whilst decreased in S2 soils (~25 and 21% lower in S2-100 and −1000 respectively) (Table 2). The number of aerobic bacterial spores decreased in S1-100 and −1000 (~12 and 26% respectively), while in S2 remained mostly unaffected (Table 2). Counts of total actinomycetes highlighted an increase in spiked S1 soils (~45% in average), while a significant decrease was noticed in S2-1000 (~30%).

355 **Table 2. Counts of heterotrophic microorganisms, Biolog average well colour**
356 **development (AWCD) and richness (no. C sources metabolised; OD_{590} > 0.15) and**
357 **DHG activity values recorded for the different soils. For each parameter, and only**
358 **within the same soil type (i.e. S1 and S2), different letters denote statistically**
359 **significant differences (*P* < 0.05).**

Soils[a]	Bacteria (Log CFU)	Fungi (Log CFU)	Actinomycetes (Log CFU)	Aerobic bacterial spores (Log CFU)	AWCD	Richness	DHG (TPF g^{-1} so
S1 control	7.09 ± 0.05^{b}	3.61 ± 0.04^{a}	6.48 ± 0.08^{a}	6.21 ± 0.05^{b}	0.175 ± 0.02^{b}	8.0 ± 0.0^{b}	24.56 ± 0.3
S1-100	6.96 ± 0.05^{a}	3.91 ± 0.10^{b}	6.70 ± 0.14^{b}	6.15 ± 0.02^{ab}	0.123 ± 0.00^{a}	6.6 ± 1.16^{a}b	20.84 ± 1.6
S1-1000	6.88 ± 0.03^{a}	3.98 ± 0.08^{b}	6.58 ± 0.05^{ab}	6.08 ± 0.04^{a}	0.088 ± 0.02^{a}	5.0 ± 1.0^{a}	21.74 ± 0.1
S2 control	5.63 ± 0.08^{a}	4.16 ± 0.04^{b}	5.31 ± 0.03^{b}	4.80 ± 0.08^{a}	0.095 ± 0.03^{a}	5.0 ± 2.0^{a}	3.66 ± 0.11
S2-100	5.82 ± 0.02^{b}	4.03 ± 0.05^{a}	5.33 ± 0.05^{b}	4.79 ± 0.03^{a}	0.067 ± 0.0^{a}	3.5 ± 0.6^{a}	7.34 ± 0.92
S2-1000	5.81 ± 0.01^{b}	4.05 ± 0.03^{a}	5.15 ± 0.05^{a}	4.81 ± 0.09^{a}	0.184 ± 0.05^{b}	6.2 ± 2.0^{a}	9.61 ± 3.24

360 a
361 S control, uncontaminated soils; S-100 and S-1000, soils spiked with 100 and 1000 mg
362 Sb(V) kg^{-1} soil respectively.

363 The high concentration of labile antimony in S1 could explain the decrease of total bacterial
364 number and aerobic bacterial spores in this soil. This may be due to a toxic effect of Sb against
365 soil bacteria as previously reported (Wang et al., 2011) and, interestingly, it was not
366 significantly influenced by the Sb concentration added. On the other hand, the increase of fungi
367 in the presence of Sb suggested that this microbial group took advantage by the bacterial
368 decrease. This was likely due to a substantial decrease of the competitive pressure exerted by
369 bacteria against fungi, as pointed out by Rousk et al. (2008). Total actinomycetes were
370 apparently unaffected by Sb (Table 2), even if Wang et al. (2011) reported a significant
371 increase of this microbial group after addition of up to 2000 mg Sb(V) kg^{-1} soil. Despite the
372 substantial concentrations of labile Sb also recorded in S2 spiked soils (which were however
373 significantly lower compared to S1 treated soils), a significant increase of readily culturable
374 bacteria was observed in this case (Table 2). This was difficult to explain, since soil bacteria
375 are commonly negatively affected by critical levels of labile PTTE (e.g. Garau et al., 2017,
376 2019a; Jiang et al., 2019) which can bind to cell enzymes compromising their function, and
377 leading to microbial death (Nannipieri, 1994; Pan and Yu, 2011). However, a significant
378 increase of substrate-induced respiration (SIR) was recorded by Guillamot et al. (2014) in soils
379 added with 50, 500 and 5000 mg kg^{-1} of Sb_2O_3. Since SIR is well correlated with the active soil
380 microbial biomass (e.g. Anderson and Domsch, 1978), this could indicate an increase of
381 soil microorganisms after Sb spiking. Moreover, Wang et al. (2011) recorded an increase of
382 culturable actinomycetes, i.e. between 50 and 150%, after the addition to soil of 2000 and
383 500 mg kg^{-1} of Sb(V) respectively, which was attributed by the authors to the selection (and
384 enrichment) of Sb-resistant microbial populations in spiked soils. This could also reasonably
385 explain the increased bacterial number in our S2 spiked soils. Sb-resistant bacterial
386 communities, able to use in a more effective way the available "food" resources, could have
387 become dominant in S2 spiked soils at the expense of Sb-sensitive ones. Moreover, the

concentration of labile Sb fractions in the more acidic S2 soil was significantly lower compared to S1, especially for S2-1000. This could have contributed to an easier adaptation to Sb of culturable bacteria in S2 due to a lower environmental pressure. Finally, the distinct responses to Sb(V) spiking suggest that microbial communities of S1 and S2 soils could be different not only in size but also in their structure.

3.3. Influence of Sb on the biolog community level physiological profile and soil dehydrogenase activity

The Biolog CLPP showed that microbial populations extracted from S1 polluted soils (after three months since spiking) had significantly reduced AWCD values compared to control soil, i.e. ~ 30 and 50% for S1-100 and −1000, respectively (Table 2). The same trend was recorded for richness values (Table 2). A significant AWCD increase (~2-fold) was instead recorded in S2-1000 soil, while richness did not change in this soil after Sb(V) addition (Table 2). In both soils, the AWCD showed the same trend of culturable heterotrophic bacteria, especially in S1 soil. This was somehow expected since fast-growing culturable bacteria were recognised as the most relevant contributors of colour development in Biolog EcoPlates™ (e.g. Garau et al., 2007; Preston-Mafham et al., 2002). The PCA analysis of C-source utilisation, capturing more than 50% of the total observed variance in the first two PCs, also indicated a clear separation (mainly along the first principal component) of the microbial communities on unpolluted S1 and S2 soils and a substantial impact of Sb(V) on C-source utilisation of both microbial communities (Fig. S1).

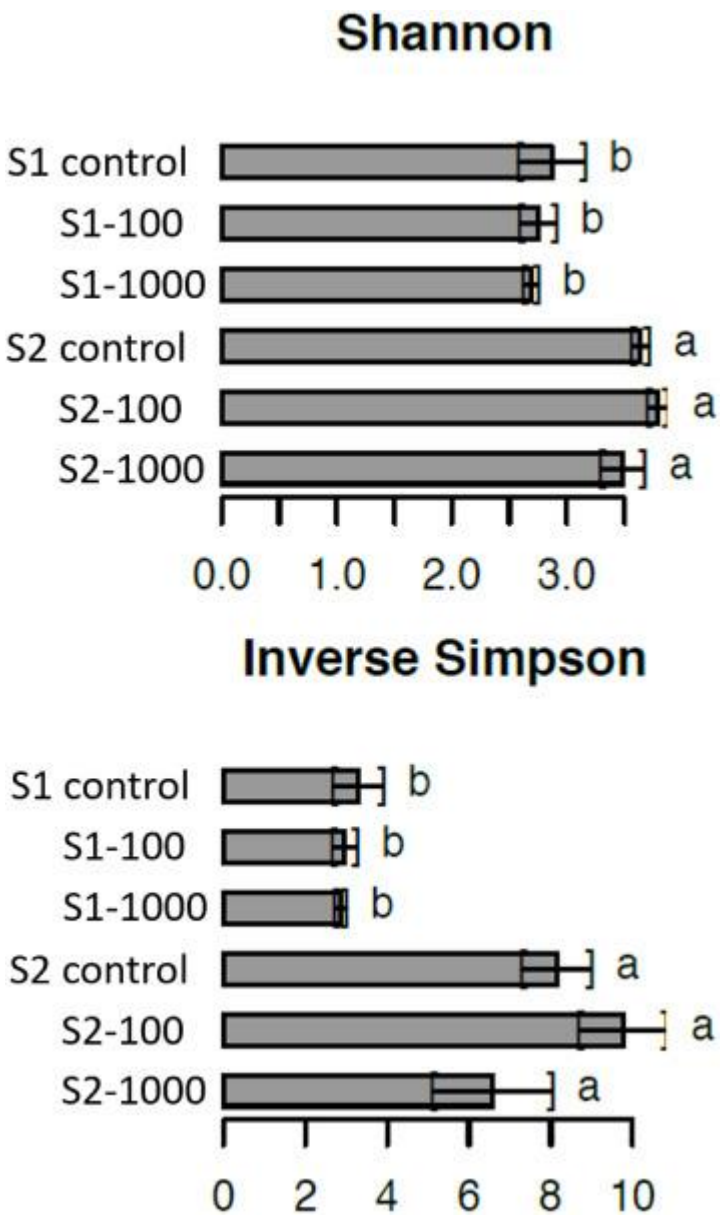
Microbial DHGs are involved in many redox processes occurring within active cells, e.g. the biological oxidation of soil organic matter or the degradation of organic xenobiotics (Wolińska and Stępniewska, 2012), and as such they have been often used as indicators of soil microbial activity (Nannipieri et al., 2003; García et al., 1997; Garau et al., 2019a, 2019b). DHG

significantly decreased in spiked S1 soils (by approx. 15 and 11% for Sb-100 and -1000 respectively), while it significantly increased in S2 soils treated with Sb(V) (approx. 2- and 2.6-fold for Sb-100 and -1000 respectively) (Table 2). In principle, labile PTTE should reduce soil enzyme activities due to their interaction with the enzyme-substrate complex, denaturation of the enzyme or interaction with the protein-active groups (Nannipieri, 1994). Labile PTTE could also affect the enzyme synthesis by means of a direct cellular toxicity, which implies a reduced number of microorganisms (Pan and Yu, 2011). On the contrary, the proliferation of PTTE-resistant microbial communities in a contaminated environment could lead to an increased enzyme synthesis. This seems indeed our case as DHG values consistently followed the number of soil heterotrophic bacteria, which was in turn governed by the antimony speciation and the physico-chemical properties of the soils. We couldn't find in literature a DHG increase after Sb addition to soil (as in the case of S2) but Murata et al. (2005) reported that 25–250 μM Sb did not affect soil DHG. On the contrary (similarly to what observed in our S1 soils), An and Kim (2009) recorded comparable DHG reductions after Sb addition to soil in the 200–1000 mg kg^{-1} range.

3.4. Sb impact on α- and β-diversity of total soil bacterial community

A total of 704,920 sequence read pairs were obtained for the 17 sequenced 16S rRNA gene amplicon sets (Table S1) (one sample of the S2-100 treatment failed at sequencing). Quality trimming, amplicon sequence reconstruction and associated quality filtering, and chimeras and aspecific amplicon removal resulted in the reduction of this number by ~30% to 499,015 analyzed high quality amplicon sequences. The per sample average sequence numbers analyzed were 29,354 (±6146) which were enough to uncover more than 99.9% of the existing diversity given the methods used, for operational taxonomic units with equal or more than relative 0.1% participation in at least 3 samples, according to the Good's coverage estimate

436 throughout all 17 samples (Table S1). The α-diversity analysis showed statistically significant
437 differences between the two soils concerning the low and intermediate dominance 0.03 distance
438 defined OTUs as indicated by the Shannon and the inverse Simpson indices respectively, but
439 no differences concerning richness (*S*), estimated richness (ACE) and highly dominant OTUs
440 (Fisher's α) as shown in Fig. 2 and Fig. S2.



441

442 **Fig. 2. Shannon and Inverse Simpson α-diversity indices of total bacterial**
443 **communities (identified OTUs) inhabiting the uncontaminated and Sb(V)-spiked**
444 **soils. S control, uncontaminated soils; S-100 and S-1000, soils spiked with 100 and**

1000 mg Sb(V) Kg^{-1} soil respectively. Different letters on top of each bar denote statistically significant differences ($P < 0.05$).

Overall, this suggested a greater bacterial diversity in the acidic S2 soil. This is remarkable since a positive correlation between soil pH and microbial diversity was highlighted in several studies (e.g. Na et al., 2018; Guo et al., 2019; Ke et al., 2019; Lin et al., 2019; Wang et al., 2020). Interestingly, after three months since spiking, the Sb(V) addition did not influence the α-diversity of bacterial communities within each soil type (not shown). This was somehow unexpected since the exposure to stressor, i.e. high PTTE concentrations, was often associated to a reduced microbiome α-diversity (e.g. Rocca et al., 2019; Hemmat-Jou et al., 2018). However, this could have occurred in our soils right after Sb(V) addition, but likely disappeared with time and/or the progressive adaptation of the bacterial communities to Sb, i.e. after the selection of phylogenetically different Sb-resistant bacterial strains. Eventually, this could also lead to increased α-diversity in PTTE-contaminated soils as previously reported (e.g. Vasileiadis et al., 2015; Hong et al., 2015). β-diversity, i.e. the community structure of soil bacteria inhabiting the different soils, was analyzed by means of PCA and its canonical version (RDA). In both cases, there was a clear distinction between the two soils. The overall model variance coincided with 97.6% of the observed variance ($P = 0.001$) and was partitioned by 93.1% and 6.9% for the soil and Sb treatment parameters respectively (Fig. 3). Both these factors were statistically significant, with the treatment associated differences being attributed to the S2 soil, that had distinct compositions between treatments as shown when the two soils were analyzed separately (Fig. S3). For soil S1, although there is apparent separation between treatment groups when considering the microbial community structures, the observed differences were not significant according to the performed PERMANOVA test ($P = 0.193$; Fig. S3). This was also apparent at the PCA plots (Fig. S4) where there was overlap along the main and secondary components between groups. On the other hand, the S2 soil

demonstrated clear treatment-wise microbial community structural differences (Fig.s 3 and S3). These results, together with those arising from culturable bacterial counts, suggest that a generalised short-term toxic effect of antimony towards the great majority of the bacterial taxa could have occurred in soil S1, as indicated by the invariance of the community structure (Fig. 3) and by the significant reduction of culturable bacteria in Sb(V)-spiked S1 soils (Table 2). On the contrary, an Sb-driven selection of certain bacterial taxa, which competitively multiplied in the Sb-contaminated soils, could have occurred in S2, as indicated by the change of the community structure (Fig. 3) and by the significant increase of culturable bacteria in Sb(V)-spiked S2 soils (Table 2). However, this view needs further confirmation as culturable bacteria are only a small (yet ecologically-relevant) part of total bacteria in soil (~1–10%; Nannipieri et al., 2017) and their behaviour could be quite different. For instance, the C-source utilisation data suggested a certain Sb impact on the structure of S1 culturable microbial community (Fig. S1), which however was not revealed by the molecular analysis of the whole soil bacterial community (likely because of a dilution effect).

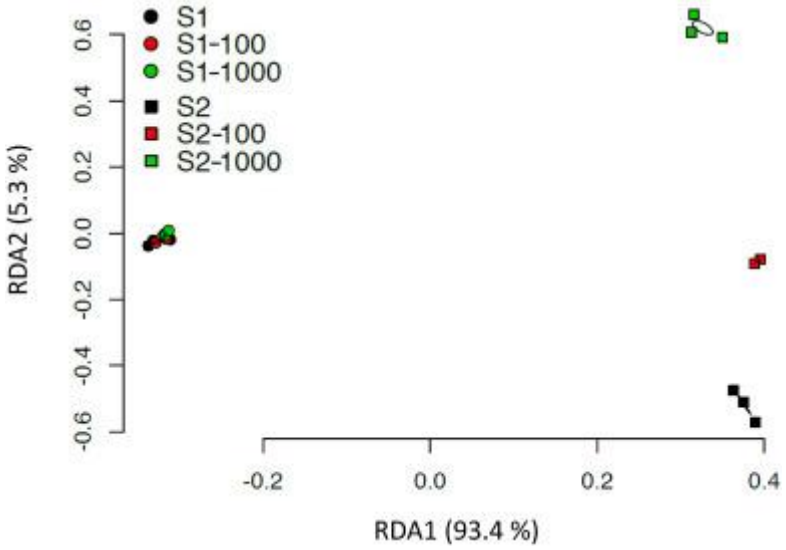


Fig. 3. Redundancy analysis (RDA) scatter plot with ellipses depicting the soil/treatment-wise sample grouping standard deviations. The model variance was 97.6% (partitioned by 93.1 and 6.9% for the soil and Sb parameters) of the observed

variance (P = 0.001). The percentages of the plotted canonical variance are provided next to the axes. S, uncontaminated soils; S-100 and S-1000, soils spiked with 100 and 1000 mg Sb(V) Kg^{-1} soil respectively.

Differential abundance tests were carried out in a treatment-wise manner for the two soils individually (given their large differences). For both soils, the performed differential abundance tests did not show strong differences between the treatments. If a *P*-value adjustment was implemented (as frequently performed in multiple-hypothesis testing) for the performed tests, all obtained *P*-values were becoming non-significant. However, the correction approaches are usually biased by the number of the participating OTUs and could therefore mask existing real differences.

Given the above, the S1 treatment-wise differentially abundant OTUs with relative abundances of 0.1% and above were only 4, which were mainly inhibited by the Sb spiking except for *Adhaeribacter* spp. (Fig.s 4 and S5). The S2 soil showed over 60 OTUs which were differently affected by the treatments (Fig.s 5 and S6). There were OTUs that were reduced in relative abundances with the Sb increase, OTUs that had hump-shape responses along the increase or decrease of the total Sb concentration and OTUs that were increased in relative abundance with the Sb increase (Fig.s 5 and S6). Interestingly, the relative abundances of taxonomic chemolithoautotrophic groups participating in the rate limiting step of nitrification (i.e. the oxidation of NH_4^+ to NO_2^-), like the β-proteobacterial *Nitrosospira* spp. and the thaumarchaeotal *Candidatus Nitrosocosmicus* spp. increased at the high Sb concentrations, whereas *Nitrospira* spp., considered as putative mixotrophs able to carry out complete ammonia oxidation (Commamox), showed reduction with increasing Sb concentrations.

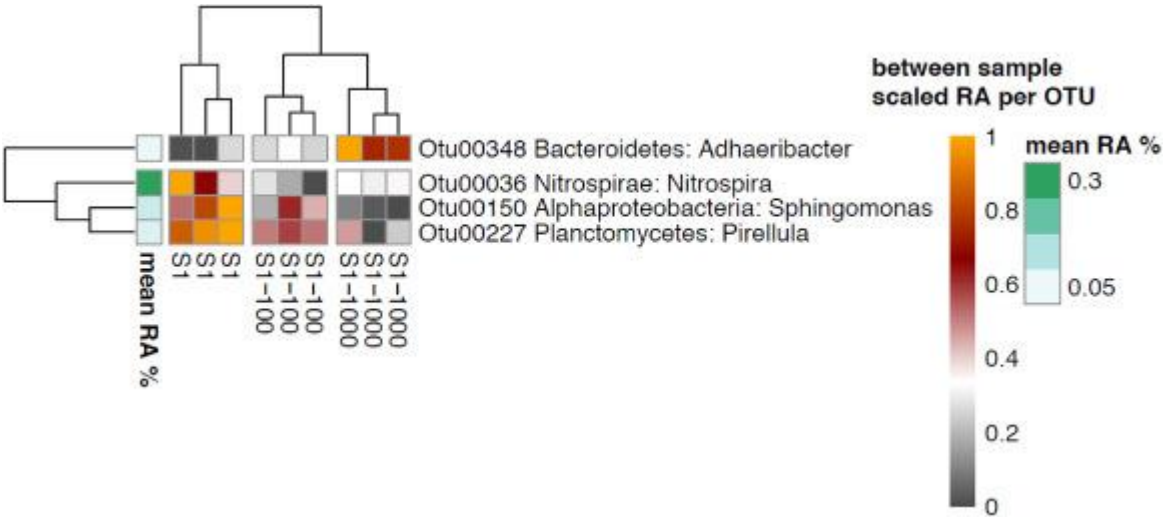


Fig. 4. Heatmap of the OTU relative abundances scaled from 0 to 1 (grey to orange key) for each differentially abundant OTU (α of 0.05; *P*-values not adjusted) for the S1 soil samples. The mean relative abundance of each OTU is indicated by the white-to-green column and key. Hierarchical clustering dendrograms are also provided. (For interpretation of the references to colour in this figure legend, the reader is referred to the Web version of this article.)

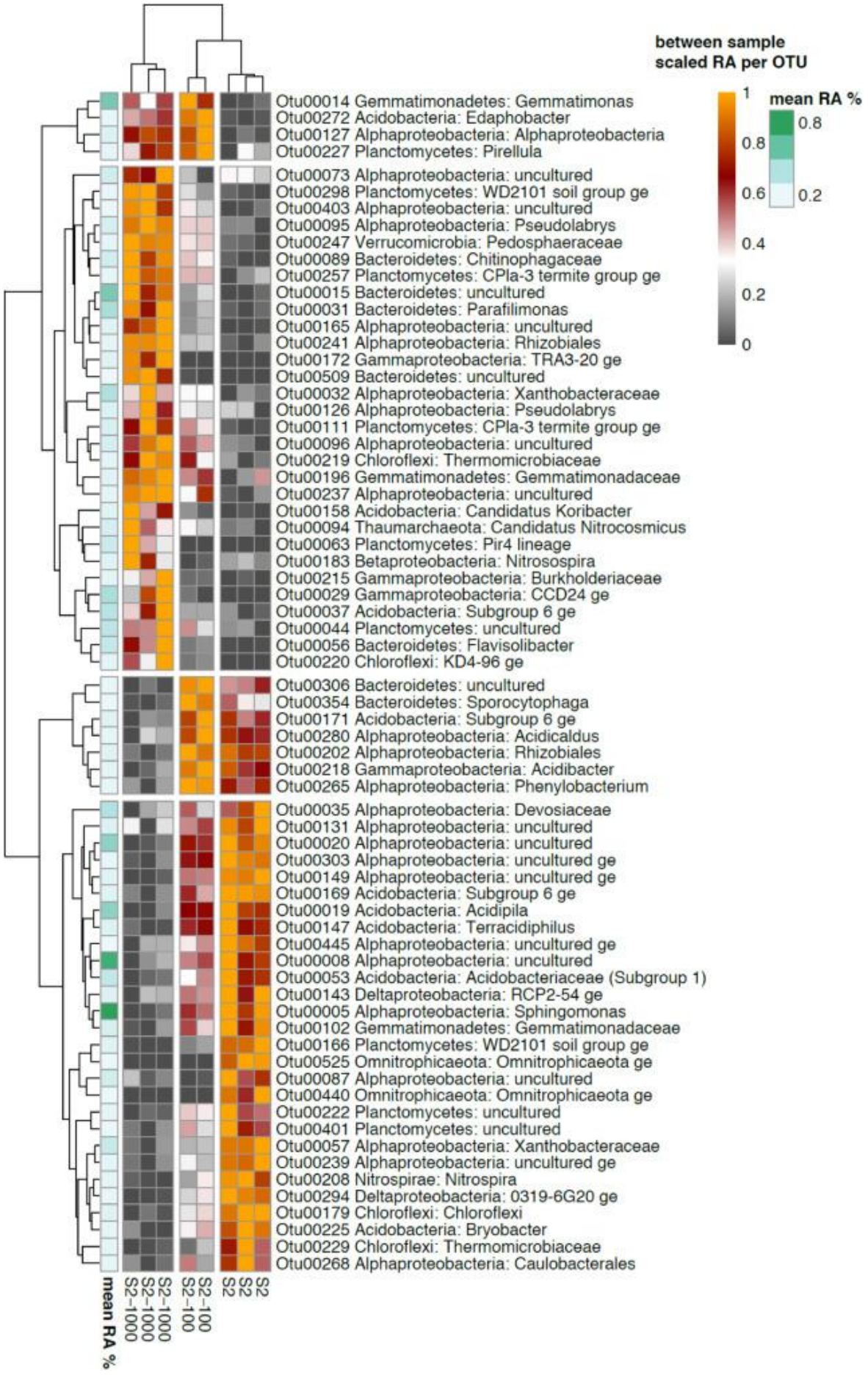

between sample
scaled RA per OTU
1
0.8
0.6
0.4
0.2
0
mean RA %
0.8
0.2
Otu00014 Gemmatimonadetes: Gemmatimonas
Otu00272 Acidobacteria: Edaphobacter
Otu00127 Alphaproteobacteria: Alphaproteobacteria
Otu00227 Planctomycetes: Pirellula
Otu00073 Alphaproteobacteria: uncultured
Otu00298 Planctomycetes: WD2101 soil group ge
Otu00403 Alphaproteobacteria: uncultured
Otu00095 Alphaproteobacteria: Pseudolabrys
Otu00247 Verrucomicrobia: Pedosphaeraceae
Otu00089 Bacteroidetes: Chitinophagaceae
Otu00257 Planctomycetes: CPla-3 termite group ge
Otu00015 Bacteroidetes: uncultured
Otu00031 Bacteroidetes: Parafilimonas
Otu00165 Alphaproteobacteria: uncultured
Otu00241 Alphaproteobacteria: Rhizobiales
Otu00172 Gammaproteobacteria: TRA3-20 ge
Otu00509 Bacteroidetes: uncultured
Otu00032 Alphaproteobacteria: Xanthobacteraceae
Otu00126 Alphaproteobacteria: Pseudolabrys
Otu00111 Planctomycetes: CPla-3 termite group ge
Otu00096 Alphaproteobacteria: uncultured
Otu00219 Chloroflexi: Thermomicrobiaceae
Otu00196 Gemmatimonadetes: Gemmatimonadaceae
Otu00237 Alphaproteobacteria: uncultured
Otu00158 Acidobacteria: Candidatus Koribacter
Otu00094 Thaumarchaeota: Candidatus Nitrocosmicus
Otu00063 Planctomycetes: Pir4 lineage
Otu00183 Betaproteobacteria: Nitrosospira
Otu00215 Gammaproteobacteria: Burkholderiaceae
Otu00029 Gammaproteobacteria: CCD24 ge
Otu00037 Acidobacteria: Subgroup 6 ge
Otu00044 Planctomycetes: uncultured
Otu00056 Bacteroidetes: Flavisolibacter
Otu00220 Chloroflexi: KD4-96 ge
Otu00306 Bacteroidetes: uncultured
Otu00354 Bacteroidetes: Sporocytophaga
Otu00171 Acidobacteria: Subgroup 6 ge
Otu00280 Alphaproteobacteria: Acidicaldus
Otu00202 Alphaproteobacteria: Rhizobiales
Otu00218 Gammaproteobacteria: Acidibacter
Otu00265 Alphaproteobacteria: Phenylobacterium
Otu00035 Alphaproteobacteria: Devosiaceae
Otu00131 Alphaproteobacteria: uncultured
Otu00020 Alphaproteobacteria: uncultured
Otu00303 Alphaproteobacteria: uncultured ge
Otu00149 Alphaproteobacteria: uncultured ge
Otu00169 Acidobacteria: Subgroup 6 ge
Otu00019 Acidobacteria: Acidipila
Otu00147 Acidobacteria: Terracidiphilus
Otu00445 Alphaproteobacteria: uncultured ge
Otu00008 Alphaproteobacteria: uncultured
Otu00053 Acidobacteria: Acidobacteriaceae (Subgroup 1)
Otu00143 Deltaproteobacteria: RCP2-54 ge
Otu00005 Alphaproteobacteria: Sphingomonas
Otu00102 Gemmatimonadetes: Gemmatimonadaceae
Otu00166 Planctomycetes: WD2101 soil group ge
Otu00525 Omnitrophicaeota: Omnitrophicaeota ge
Otu00087 Alphaproteobacteria: uncultured
Otu00440 Omnitrophicaeota: Omnitrophicaeota ge
Otu00222 Planctomycetes: uncultured
Otu00401 Planctomycetes: uncultured
Otu00057 Alphaproteobacteria: Xanthobacteraceae
Otu00239 Alphaproteobacteria: uncultured ge
Otu00208 Nitrospirae: Nitrospira
Otu00294 Deltaproteobacteria: 0319-6G20 ge
Otu00179 Chloroflexi: Chloroflexi
Otu00225 Acidobacteria: Bryobacter
Otu00229 Chloroflexi: Thermomicrobiaceae
Otu00268 Alphaproteobacteria: Caulobacterales
mean RA %
S2−1000
S2−1000
S2−1000
S2−100
S2−100
S2−100
S2
S2
S2

Fig. 5. Heatmap of the OTU relative abundances scaled from 0 to 1 (grey to orange key) for each differentially abundant OTU (α of 0.05; *P*-values not adjusted) for the S2 soil samples. The mean relative abundance of each OTU is indicated by the white-to-green column and key. Hierarchical clustering dendrograms are also provided. (For interpretation of the references to colour in this figure legend, the reader is referred to the Web version of this article.)

Pearson correlation tests were performed for identifying OTUs responsive in relative abundances to the different Sb pools recovered with the sequential extraction in S1 and S2 soils. Due to the multicollinearity of the different Sb pools recovered with the sequential extraction (Pearson correlation *r* values of 0.99–1, *P*-values = 0), the water-soluble Sb was used in the correlation tests given its high environmental relevance. The analysis confirmed that the relative abundances of taxonomic groups participating in the rate limiting step of nitrification

(e.g. *Nitrosophaeraceae*, $r = 0.61$, $P = 0.01$; *Nitrosospira* spp., $r = 0.48$, $P = 0.049$) correlated positively with the water-soluble Sb pools (Fig. S7) as highlighted by the performed correlation test. Moreover, the relative abundance of other microbial phyla was found positively and highly correlated with water-soluble Sb, e.g. *Adhaeribacter* spp. ($r = 0.72$, $P = 0.001$), *Blastopirellula* spp. ($r = 0.57$, $P = 0.018$) and *Tumebacillus* spp. ($r = 0.75$, $P < 0.001$) (Fig. S7).

4. Conclusions

The results obtained indicated that the behaviour of Sb after three months since spiking, i.e. its mobility and toxicity, was significantly affected by the soil physico-chemical properties, such as the pH and the content of clay, organic matter and Al and Fe hydroxides. In this regard, the pH seemed to play the main role in regulating the concentration of labile Sb in soil.

Despite substantial amounts of labile Sb were present in both soils, the contaminant influence on culturable microbial communities was different encompassing stimulating and repressive effects (e.g. bacteria in S2 and S1 respectively). The same trend was confirmed for both soils by the Biolog CLPP as well as by the soil DHG activity. This could be attributed to the presence of different microbial populations in the two soils which responded differently to the Sb stress. This view was supported by the Illumina amplicon sequencing which also showed that Sb contamination could have a stimulating effect on some bacterial taxa participating in the rate-limiting step of nitrification.

Overall, the results obtained suggest that the risk assessment in soils polluted with antimony should be a priority especially for alkaline soils, where the high mobility of the anionic $Sb(OH)_6^-$ species can represent a serious threat for soil microbial abundance, diversity and functionality, as well as for soil fertility and eventually human health. Finally, our results suggest that soil microbial and biochemical data should be considered for a thorough assessment of the environmental risk related to Sb contamination.

CRediT authorship contribution statement

Stefania Diquattro: Investigation, Formal analysis, Writing - original draft. **Giovanni Garau:** Conceptualization, Methodology, Writing - review & editing. **Nicoletta P. Mangia:** Investigation. **Barbara Drigo:** Investigation. **Enzo Lombi:** Resources, Writing - review & editing. **Sotirios Vasileiadis:** Investigation, Formal analysis, Writing - original draft. **Paola Castaldi:** Conceptualization, Methodology, Writing - original draft, Supervision.

Declaration of competing interests

The authors declare that they have no known competing financial interests or personal relationships that could have appeared to influence the work reported in this paper.

Acknowledgements

The authors would like to the thank the University of Sassari (Italy) that financially contributed to this study with the “Fondo di Ateneo per la Ricerca 2019”.